

The Effect of Grain Boundary Sliding and Strain Rate Sensitivity on the Ductility of Ultrafine-Grained Materials

Nguyen Q. Chinh^{1,a}, Tamás Csanádi^{1,b}, Jenő Gubicza^{1,c}
Ruslan Z. Valiev^{2,d}, Boris B. Straumal^{3,4,e}, Terence G. Langdon^{5,6,f}

¹ Department of Materials Physics, Eötvös Loránd University, H-1117 Budapest, Hungary

² Institute of Physics of Advanced Materials, Ufa State Aviation Technical University, Ufa 450000 Russia

³ Institute of Solid State Physics, Russian Academy of Sciences, Chernogolovka, Moscow district, 142432 Russia

⁴ Max-Planck-Institut für Metallforschung, 70569 Stuttgart, Germany

⁵ Departments of Aerospace & Mechanical Engineering and Materials Science, University of Southern California, Los Angeles, CA 90089-1453, USA

⁶ Materials Research Group, School of Engineering Sciences, University of Southampton, Southampton SO17 1BJ, U.K.

^achinh@metal.elte.hu, ^bcsanadi@metal.elte.hu, ^cgubicza@metal.elte.hu, ^drzvaliev@mail.rb.ru, ^estraumal@issp.ac.ru, ^flangdon@usc.edu

Keywords: Ultrafine-grained materials, grain boundary sliding, wetted boundaries, strain rate sensitivity, ductility

Abstract. Most ultrafine-grained (UFG) materials produced by severe plastic deformation (SPD) exhibit only limited ductility which is correlated with the low strain rate sensitivity (SRS) of these materials. Recently, it was demonstrated that SPD is capable of increasing the room temperature ductility of aluminum-based alloys attaining elongations up to 150%, together with relatively high strain rate sensitivity. In the present work, additional results and discussions are presented on the effect of grain boundary sliding (GBS) and SRS on the ductility of some UFG metals and alloys. The characteristics of constitutive equations describing the steady-state deformation process are quantitatively analyzed for a better understanding of the effects of grain boundaries and strain rate sensitivity.

Introduction

Ultrafine-grained (UFG) materials can be mostly achieved by using severe plastic deformation (SPD) techniques such as equal-channel angular pressing (ECAP) or high-pressure torsion (HPT) [1-3] methods. As a consequence of the severe deformation, in general, the UFG materials have reasonably saturated microstructures with a steady-state dislocation density [4]. Under these conditions, the role of the grain boundaries is enhanced in the post-SPD deformation processes. There are both indirect and direct evidences suggesting that grain boundary sliding (GBS) may occur more easily at room temperature (RT) in UFG metals [5] and this may lead to reasonable levels of tensile ductility. However, the most SPD-processed materials exhibit only limited ductility, which is unambiguously correlated with the low strain rate sensitivity (SRS) of these materials [6]. Recently, we demonstrated the room temperature super-ductility of a UFG Al-30Zn alloy in which GBS takes place with relatively high SRS [7]. In this work, the effect of GBS taking place in different materials is discussed and related to the SRS. Additional results are presented to demonstrate the role of diffusion-controlled GBS on the ductility of UFG materials.

Experimental materials and procedures

The experiments were conducted on high purity face-centered cubic (fcc) metals (Al, Ag and Cu), the Zn-22%Al eutectoid alloy and an Al-30%Zn aluminum alloy. The pure metal and eutectoid samples were processed by ECAP to have the saturation state with UFG structures. More details are reported elsewhere for Al [5,8], Ag [9], Cu [8,10] and Zn-22%Al [11,12] samples, respectively. The microstructure of Al-30Zn samples processed by HPT contains equiaxed ultrafine Al grains having a size of ~380 nm with smaller Zn grains located at the triple junctions of the Al grains and this leads to a wetting of the Al/Al grain boundaries [7]. More details on the principles of processing by ECAP and HPT were given in earlier reports [1-3].

Depth-sensing indentation (DSI) tests with a Vickers indenter and atomic force microscopy (AFM) measurements were made to identify the mechanism of plastic deformation. DSI measurements were carried out with a Vickers microindenter operating under a force, F , that increased linearly with time, t , by an imposed loading rate, ν , between 0.7 and 70 mN s⁻¹. It may be estimated from an earlier analysis [13] that the equivalent strain rate, $\dot{\epsilon}_{eq}$, around the edge of the indenter at the end of the indentation process is proportional to the the loading rate. After indentation, the changes in the surface topographies were examined around the indentations using AFM. Full details of these investigations were reported earlier [5,7].

Experimental results and discussion

In recent work [4] it was shown for fcc metals that there is a saturation of the flow stress at very high strains which is the result of a dynamic equilibrium between the formation and annihilation of dislocations. In the saturation stage, despite the relatively low temperature (RT) of deformation, the behavior is similar to the flow process in the steady-state stage of creep where the annihilation of dislocations is controlled by dislocation climb. It was observed that the room temperature saturation stress, σ_{sat} , of fcc metals can be scaled to the absolute melting point, T_m , in the form:

$$\frac{\sigma_{sat}}{\mu} = K \cdot \exp\left(\frac{A \cdot T_m}{R \cdot T}\right) \quad (1)$$

where μ is the shear modulus, $K = 1.25 \cdot 10^{-3}$, $A = 3.46 \text{ J} \cdot \text{K}^{-1} \cdot \text{mole}^{-1}$, R is the universal gas constant and T is the absolute testing temperature. This relationship also suggests that the plastic process at the saturation flow stress may be described through the relationship generally applied in steady-state creep:

$$\dot{\epsilon} = K_1 \cdot \sigma_{sat}^{1/m} \cdot \exp\left(-\frac{Q}{RT}\right), \quad (2)$$

where $\dot{\epsilon}$ is the strain rate, m is the strain rate sensitivity, Q is the activation energy characterizing the deformation process and K_1 is a microstructure-dependent constant for a given metal. Assuming a constant strain rate, eq. (2) may be expressed as

$$\sigma_{sat} = K_2 \cdot \exp\left(\frac{mQ}{RT}\right), \quad (3)$$

where K_2 is another constant.

According to eqs. (2) and (3), the values of m and Q can be determined from the slope of the straight lines fitted to the $\ln \dot{\epsilon} - \ln \sigma$ data obtained at a given temperature and to the $\ln \sigma - 1/T$ data obtained at a constant strain rate, respectively. In general, the strain rate, $\dot{\epsilon}$, and stress, σ , obtained by uniaxial tensile or compression tests are used in eqs. (2) and (3), as was applied for UFG Al in earlier work [14]. In the present case, using the proportionality between the Vickers hardness, HV

and the flow stress, σ , as well as the proportionality between the equivalent strain rate, $\dot{\epsilon}_{eq}$, and the loading rate, v , during indentation, instead of the conventional $\ln \dot{\epsilon} - \ln \sigma$ and $\ln \sigma - 1/T$ connections, the $\ln v - \ln HV$ and $\ln HV - 1/T$ relationships are used for the analysis. As a demonstration of the application of the indentation measurements, Fig. 1 shows a set of these relationships to give experimental values of m and Q for Al-30Zn alloy in the cases of both conventional and UFG Al-30Zn alloys.

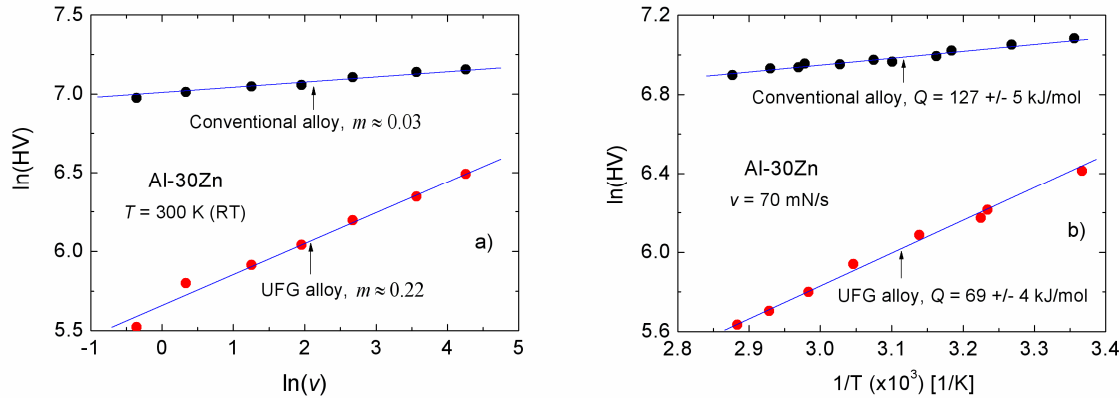


Figure 1: An evaluation of a) the strain rate sensitivity, m , and b) activation energy, Q , for Al-30Zn alloys (HV given in MPa and v in mN/s).

Table 1 contains the values of m and Q obtained around RT (Q was determined in the temperature range between 300 and 350K) for different materials, including also the conventional Al-30Zn and eutectoid Zn-22Al which is a model alloy showing superplasticity at high temperatures. Experimental results show that the value of the activation energy of each SPD processed material is near to that for grain boundary diffusion, Q_{gb} , in these materials.

Table 1: The values of m and Q for some metals and alloys tested at RT

Material	Grain size [nm]	Test	Strain rate sensitivity m	Activation energy Q [kJ/mole]	Ductility [%]
ECAP Al	~ 1200 [5,8]	compression	0.030 [14]	82 [14]	< 20%
ECAP Al	~ 1200	indentation	0.026	87	
ECAP Ag	~ 200 [9]	indentation	0.022	105	
ECAP Cu	~ 300 [8,10]	indentation	0.020	107	
ECAP Zn-22Al	~ 800 [12]	indentation	0.13	75	~ 240 [12]*
Conventional Zn-22Al	~ 1800 [12]	indentation	0.086	92	~ 170 [12]*
HPT Al-30Zn	~ 380 [7]	tensile	0.24÷0.29 [7]	-	~ 150 [7]
HPT Al-30Zn	~ 380	indentation	0.22	69	super-ductility at RT
Conventional Al-30Zn	~70000 [7]	indentation	0.02	127	-

(* Both belong to high temperature deformation concerning the eutectoid samples)

These results demonstrate that, whereas at high temperatures the rate of steady-state creep is controlled by diffusion through the crystalline lattice, in the low temperature region grain boundary diffusion becomes a significant factor in determining the rate of steady-state flow. Furthermore, it

appears that at relatively low temperatures ($T < 0.5T_m$) the flow of UFG materials occurs with a significant contribution from a grain boundary process such as GBS. This explanation is also consistent with the reasonably unchanged microstructures that are observed in pure Al and aluminum-based alloys after pressing through ~ 4 passes in ECAP and then continuing to high imposed strains [15,16].

Recently, it was shown that the mechanism of grain boundary sliding can be made visible in three-dimension by using AFM [5,7,14]. Figure 2 shows the indentation patterns of an ECAP-processed Al sample deformed with a maximum load of 20 mN. It can be seen that there is a rumpling around the indentation which corresponds to the displacements of grains within the UFG matrix. It is concluded that the grains, having a size of $\sim 1.2 \mu\text{m}$, move with respect to each other. It is suggested that this representation provides good evidence for the occurrence of GBS as a significant mechanism for deformation of UFG Al at RT. Two specific grain boundaries are labeled 1 and 2 on the path designated ECAP-1 in Fig. 2 and these two boundaries are more clearly visible in the small inset shown at the upper right in Fig. 2, providing a unique and unambiguous evidence for the occurrence of extensive GBS within a narrow peripheral zone in the pure aluminum processed by ECAP and subsequently subjected to dynamic DSI testing at RT. More details of these investigations can be found elsewhere [14].

Despite the significant role of GBS, which is the main mechanism for superplastic deformation at high temperatures (where the testing temperature, T , is larger than $0.5T_m$) [17-19], the value of the SRS (m) and the ductility of the investigated pure metals (Al and Cu) is extremely small. It should be mentioned that the low value between 0.01 and 0.03 is typical for the SRS often recorded in fcc metals deformed at low temperatures [6]. Considering the plastic properties of Al alloys, the behavior of the UFG Al-30Zn processed by HPT [7] is prominent and unique, as it is possible to increase the room temperature ductility of this alloy to attain elongations to failure higher than 150%. Furthermore, the value of room temperature SRS ($m > 0.2$) is unusually high, about ten times higher than that of other metals and alloys investigated so far at RT.

The unusual room temperature mechanical behavior of UFG Al-30Zn alloy were reported recently [7]. It was shown that the unique properties are due to the special occurrence of GBS at RT. The HPT processing introduced a wetting of the grain boundaries, as the aluminum/aluminum grain boundaries are wetted by thin layers of Zn. Figure 3 shows a typical AFM image of the surface after indentation with Vickers microindenter on the UFG Al-30Zn sample. The vicinity of the Vickers pattern looks like it has been scattered by “sand-like” grains having a size of about 400 nm. Detailed measurements [7] have revealed that this rumpling picture also corresponds to the displacements of the individual ultrafine grains within the crystalline matrix.

It should be emphasized that there is not a quantitative difference in the contribution of GBS for UFG pure Al and UFG Al-30Zn materials. This contribution to the total deformation process in both

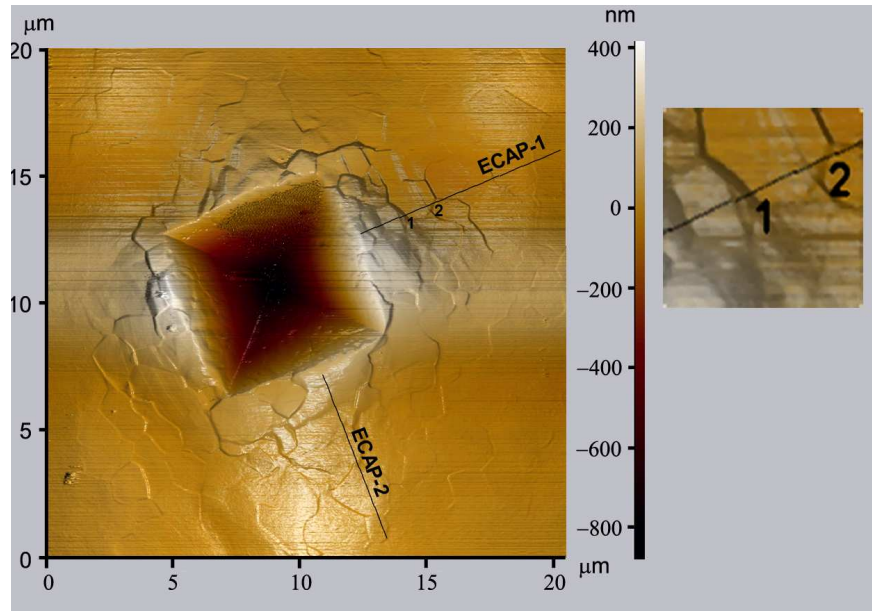


Figure 2: An AFM micrograph of the surface of the UFG pure Al sample deformed by indentation using a Vickers indenter [14].

cases is about 50-60% during the indentation [5,7]. Considering the shapes of pile-ups around the Vickers patterns shown in Figs. 2 and 3, however, one can see that there is a significant qualitative difference in GBS for these two materials. Typical vertical profiles across the Vickers microhardness patterns, plotted in Fig. 4a reveal that while the pile-ups formed in the case of UFG pure Al are rather short-term, looking sharp directly near the Vickers pattern, those observed on the UFG Al-30Zn sample appear to be long-term, spreading over relatively much longer distances from the Vickers pattern and therefore looking smooth around the pattern. This difference can be explained by the significantly higher mobility of wetted GBs containing Zn phase particles in Al-30Zn alloy, the behavior of which tends towards that of liquids, making this UFG material super-ductile at RT. Furthermore, this difference in GBS is in correlation with the values of the SRS of the two materials, as schematically demonstrated in Fig. 4b. In the case of UFG Al-30Zn alloy, because of a relatively high SRS, high pile-ups cannot form around the Vickers pattern, which is equivalent with the phenomenon in tensile testing when the strain (or stress) will not concentrate locally so that a neck is not formed. Instead, the pile-ups spread over a large area thereby homogenizing the deformation and eventually leading to the super-ductility of this alloy at RT. Physically, the higher SRS of UFG Al-30Zn hinders more effectively the local deformation in the vicinity of the Vickers pattern where the strain and the strain rate are the highest. As a consequence, the deformation spreads also over larger distances from the pattern.

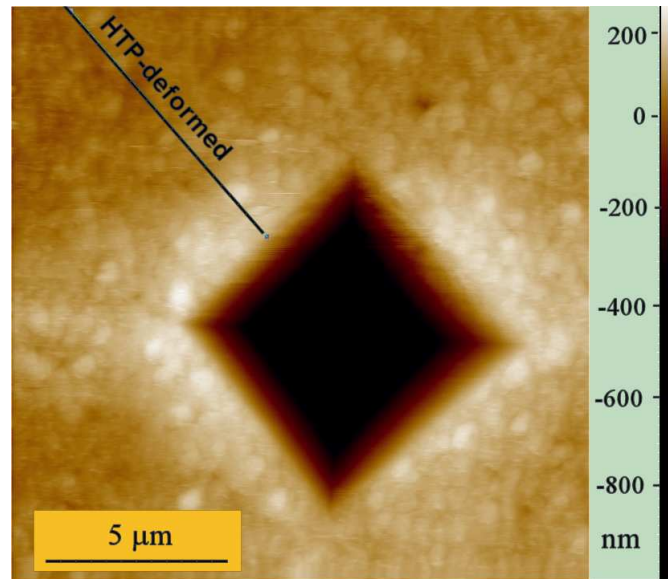


Figure 3: An AFM micrograph of the surface of the UFG Al-30Zn sample deformed by indentation using a Vickers indenter [7]

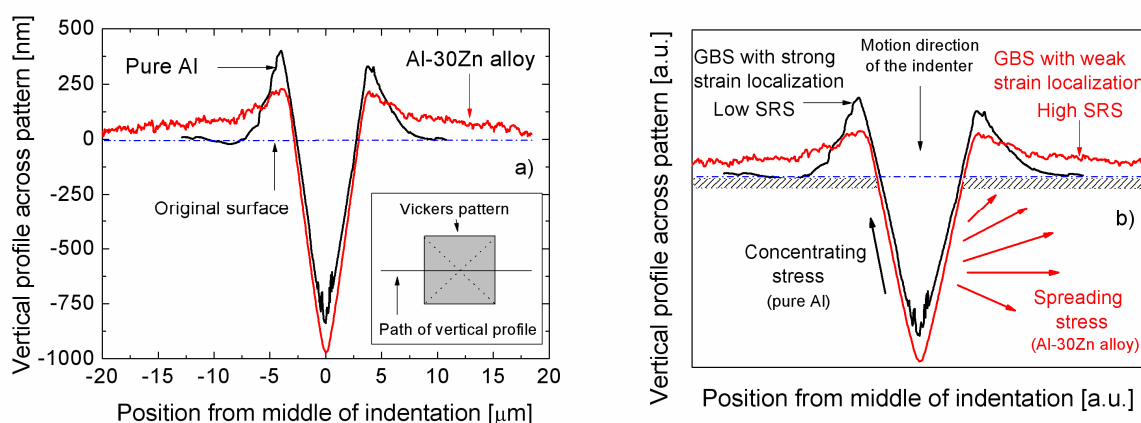


Figure 4: Plot of the vertical profiles across the centers of the Vickers patterns a) showing the qualitative difference in GBS of UFG pure Al and Al-30Zn and b) schematically demonstrating the deformation profile under the Vickers indenter and the correlation between GBS and SRS.

Considering the activation energy of 69 kJ/mole, which is lower than the values for self-diffusion in Al (142 kJ/mole [20]), for self-diffusion in Zn (92 kJ/mole [20]) and that for grain boundary diffusion in Al (84 kJ/mole [20]), it is anticipated that the deformation-controlling process in the UFG Al-30Zn alloy cannot be either the diffusion of Al or the self-diffusion of Zn. As the frequency

factor (pre-exponential), D_0 , of the diffusion coefficient, D , of these three diffusions is between $1.3 \cdot 10^{-5}$ and $1.7 \cdot 10^{-4} \text{ m}^2 / \text{s}$ [20], supposing a similar frequency factor for the room temperature diffusion process in the investigated UFG Al-30Zn alloy, a value between $1.2 \cdot 10^{-17}$ and $1.6 \cdot 10^{-16} \text{ m}^2 / \text{s}$ can be estimated for the diffusion coefficient, D , which is about three orders of magnitude higher than the coefficient ($\sim 10^{-19} \text{ m}^2 / \text{s}$) for Al self-diffusion along the Al/Al GBs. Although additional investigations are needed to study the diffusion process in the UFG Al-30Zn alloy, it should be noted that the estimated value reasonably correlates to that measured for the diffusion ($\sim 10^{-15} \text{ m}^2 / \text{s}$) of Zn along Al/Al grain boundaries [21,22], therefore suggesting that the observed superductile behaviour of the UFG Al-30Zn alloy at RT is controlled by GBS and Zn diffusion along the wetted Al/Al grain boundaries.

Summary and conclusions

The room temperature plastic deformation of metals and alloys was investigated by DSI tests and using AFM. The results show that GBS is a significant mechanism of plastic deformation even at low temperatures when the grain size is very small. Despite the strong contribution of GBS, the SRS and the ductility of UFG materials are, in general, poor because of slow diffusion in the controlling process. It is shown that an improvement of diffusion along grain boundaries, for example in the case of wetted grain boundaries, unambiguously enhances the SRS and the ductility of the UFG materials.

Acknowledgements: This work was supported by the Hungarian Scientific Research Fund (OTKA) under Grant No. K81360, K67692 and TÁMOP 4.2.1/B-09/1/KMR (NQC, JG) and by the National Science Foundation of the United States under Grant No. DMR-0855009 (TGL). In addition, NQC thanks the Hungarian-American Enterprise Scholarship Fund for support.

References

- [1] R.Z. Valiev, R.K. Islamgaliev, I.V. Alexandrov. *Prog Mater Sci* 45 (2000), p. 103
- [2] R.Z. Valiev, T.G. Langdon, *Prog. Mater. Sci.* 51 (2006), p. 881
- [3] A.P. Zhilyaev, T.G. Langdon, *Prog Mater Sci* 41 (2006), p. 597
- [4] N.Q. Chinh, T. Csanádi, G. Gubicza, T.G. Langdon, *Acta Mater*, 58 (2010), 5015
- [5] N.Q. Chinh, P. Szommer, Z. Horita, T.G. Langdon, *Adv. Mater.* 18 (2006), p. 34
- [6] M.A. Meyer, A. Mishra, D.J. Benson, *JOM* 58(4) (2006), p. 41
- [7] R.Z. Valiev, M.Y. Murashkin, A. Kilmametov, B. Straumal, N.Q. Chinh, T.G. Langdon, *J Mater Sci* 45 (2010), p. 4718
- [8] S. Komura, Z. Horita, M. Nemoto, T.G. Langdon, *J Mater. Res.* 14 (1999), p. 4044
- [9] J. Gubicza, N.Q. Chinh, J.L. Labar, Z. Hegedűs, T.G. Langdon, *Mater. Sci. Eng. A527* (2010), p. 752.
- [10] A. Vinogradov, S. Hashimono, V. Patlan, K. Kitagawa, *Mater. Sci. Eng. A319-321* (2001), p. 862
- [11] P. Kumar, C. Xu, T.G. Langdon, *Mater. Sci. Eng. A410-411* (200), p. 447
- [12] P. Kumar, C. Xu, T.G. Langdon, *Mater. Sci. Eng. A429* (2006), p 324
- [13] N.Q. Chinh, J. Gubicza, Zs. Kovács, J. Lendvai. *J Mater. Res.* 19 (2004), p. 31
- [14] N.Q. Chinh, P. Szommer, T. Csanádi, T.G. Langdon, *Mater. Sci. Eng. A434* (2006), p. 326
- [15] S.D. Terhune, D.L. Swisher, K. Oh-ishi, Z. Horita, T.G. Langdon, T.R. McNelley, *Metall. Mater. Trans.* 33A (2002), p. 2173
- [16] C. Xu, M. Furukawa, Z. Horita, T.G. Langdon, *Mater. Sci. Eng. A398* (2005), p. 66.
- [17] T.G. Langdon, *Mater. Sci. Eng. A174* (1994), p. 225.
- [18] T.G. Langdon, *J. Mater. Sci.* 41 (2006), p. 597.
- [19] T. G. Langdon, *J. Mater. Sci.* 42 (2007), p. 1782.
- [20] H.J. Frost, M.F. Ashby: *Deformation-Mechanism Maps: The Plasticity and Creep of Metals and Ceramics*. Pergamon Press, Oxford, UK (1982).
- [21] H. Mehrer (ed.), *Diffusion in Solid Metals and Alloys. Landolt-Börnstein*, Vol. 26 (Springer, Berlin etc., 1990).
- [22] I. Kaur, W. Gust, L. Kosma, *Handbook of interphase and grain boundary diffusion* (Ziegler press, Stuttgart, 1989).